Roles of Ile209 and Ile210 on the Heme Pocket Structure and Regulation of Histidine Kinase Activity of Oxygen Sensor FixL from *Rhizobium meliloti*†

Masahiro Mukai,*,‡ Kayako Nakamura,§ Hiro Nakamura,‡ Tetsutaro Iizuka,‡,|| and Yoshitsugu Shiro‡

RIKEN Harima Institute/Spring-8, Mikazuki-cho, Hyogo 679-5148, Japan, and Kyoritsu College of Pharmacy, Minato-ku, Tokyo 105-0011, Japan

Received May 24, 2000; Revised Manuscript Received September 18, 2000

ABSTRACT: FixL is a sensor histidine kinase having a heme-containing domain as an O_2 sensing site. In the study presented here, Ile209 and Ile210 located near the heme iron of the heme domain of *Rhizobium meliloti* FixL (RmFixL) were mutated, and the mutational effects on the regulation of the kinase activity and the heme pocket structure were examined by the autophosphorylation assay and UV−visible absorption and resonance Raman (RR) spectroscopies. The mutation of these residues disrupted the regulation of the kinase activity by the sensor (heme) domain, indicating that Ile209 and Ile210 play important roles in the signal transduction between the heme and the kinase domains. By measurement of the resonance Raman and optical absorption spectra of Ile209 and Ile210 mutants in several oxidation, spin, and ligation states, it was found that both residues are highly flexible, and their side chains sterically interact with the O_2 ligand, when it binds to the heme iron. On the basis of the results, we propose an O_2 sensing mechanism of RmFixL; the kinase activity is regulated via conformational changes of Ile209 and Ile210 induced by the O_2 binding to the sensory center.

The rhizobial FixL protein is a biological oxygen sensor for regulating the transcription of nitrogen fixation genes in plant root nodules (*1*−*3*). *Rhizobium meliloti* FixL (RmFixL)[1] consists of three functionally separated domains, i.e., transmembrane, oxygen sensor, and kinase domains (*4*). The kinase domain is homologous to the other sensor histidine kinases of the two-component regulatory systems (*4*, *5*). On the other hand, the sensor domain of FixL is not conserved with respect to those of other sensor histidine kinases. The sensor domain of FixL with ∼150 amino acid residues contains a heme (iron protoporphyrin). Binding of O_2 at the ferrous iron of the heme is responsible for the regulation of the kinase activity; namely, the kinase is inactive in the O_2-bound (oxy) form of the heme, while autophosphorylation with ATP in the kinase domain is activated in the O_2-unbound (deoxy) form, followed by the phosphoryl transfer to the transcriptional activator FixJ (*6*−*8*). The information about the O_2 association with or dissociation from the heme should be transmitted to the kinase domain via some structural changes in the protein.

Concerning the mechanism for the regulation of the kinase activity of FixL by the heme domain, there have been two proposals on the basis of the crystal structures of the heme domains of FixLs. First, Gong et al. reported the crystal structures of the heme domain of *Bradyrhizobium japonicum* FixL (BjFixLH) in the ferric ligand-free (met), ferric CN^--bound, ferric imidazole-bound, ferrous O_2-bound (oxy), and ferrous nitric oxide-bound forms (*9*, *10*). They observed rearrangements of the hydrogen bond network between the heme 6,7-propionates and amino acid residues (Arg206 and His214) in the F/G loop region between the met (ligand-free) and other ligand-bound forms. As the changes of the hydrogen bonds seemed to be caused by the flattening of the heme plane upon the ligand binding, they proposed that the signal transduction might be mainly driven by the motion of the heme plane induced by ligand binding.

On the other hand, Miyatake et al. (*11*) determined the crystal structure of the heme domain of the met and deoxy RmFixLH at a higher (1.4 Å) resolution and unambiguously fixed the amino acid residues located near the heme, as shown in Figure 1. The distal heme pocket is packed so densely that the O_2 ligand could not bind to the iron without serious collisions with three residues, Ile209, Leu230, and Val232. In addition, interaction between the O_2 ligand and Ile209 was suggested by the resonance Raman (RR) spectra of the I209A mutant. Therefore, they proposed the O_2 sensing mechanism in which the regulation of the kinase activity is initially driven by the steric repulsion between the O_2 ligand and Ile209. Perutz et al. have also made the same proposal based on the structural data of the met and CN-bound forms of BjFixLH; i.e., the conformational changes of the distal amino acid residues (Ile215, Leu236, and Ile238 in BjFixL, which correspond to Ile209, Leu230, and Val232 in RmFixL, respectively) near the heme iron would be transmitted to the kinase domain (*12*). They suggested that the driving force of the conformational change is steric effects between the three residues mentioned above and the iron-bound ligand.

† This work was supported by the Special Postdoctoral Researcher's Program in RIKEN (to M.M. and K.N.).

‡ RIKEN Harima Institute/Spring-8.

§ Kyoritsu College of Pharmacy.

|| Present address: Department of Materials Chemistry, Faculty of Engineering, Hosei University, Koganei, Tokyo 184-8584, Japan.

[1] Abbreviations: RmFixL, *R. meliloti* FixL; BjFixL, *B. japonicum* FixL; FixLH, heme domain of FixL; FixLT, soluble truncated FixL (consisting of the heme and kinase domains); RR, resonance Raman; WT, wild-type; UV, ultraviolet; DTT, dithiothreitol; Mb, myoglobin; 5c, five-coordinate; 6c, six-coordinate; HS, high-spin; LS, low-spin.

10.1021/bi001184x CCC: $19.00 © 2000 American Chemical Society
Published on Web 10/21/2000

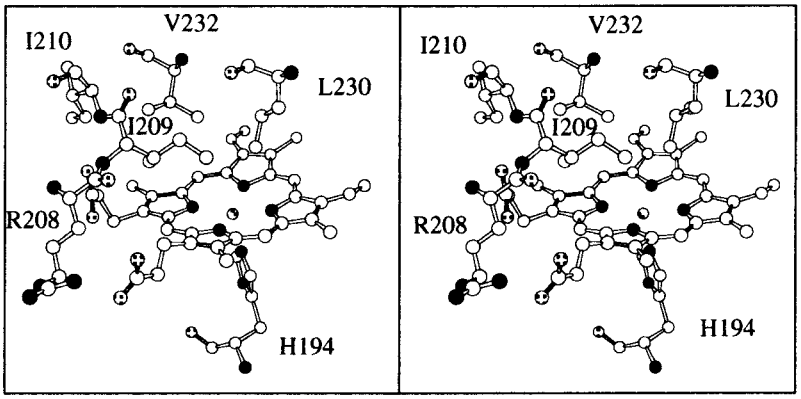

FIGURE 1: Stereoview of the heme and amino acid residues near the heme in *R. meliloti* FixL (*11*).

To elucidate the oxygen sensing mechanism, we further investigated the mutational effects of Ile209 and Ile210, which has the same effect on an autoxidation rate of the heme iron as Ile209 (*13*), on the autophosphoryl activity, the heme pocket structure, and the coordination structure of the heme in RmFixL, which consists of the heme and kinase domains (RmFixLT). We selected Ala, His, and Trp residues in expecting the hydrophilic effect with the His mutation and the size effect with the Ala and Trp mutations.

MATERIALS AND METHODS

Sample Preparation and Measurement of Autophosphorylation Activity. A soluble truncated RmFixL (consisting of the heme and the kinase domains, FixLT) and its site-directed mutants were overexpressed in *Escherichia coli* strain JM109 and purified as previously described (*13*). Measurement of the autophosphorylation activity of FixLs was carried out with a previously described method (*8*). Reaction mixtures contained 5.0 μM FixL, 0.2 mM [γ-^{32}P]ATP, and dithiothreitol (DTT) (50 mM for the deoxy form and 10 mM for the oxy form) or β-mercaptoethanol (β-ME) (50 mM for the oxy form) in the kinase buffer [10 mM KCl, 0.2 mM $MnCl_2$, and 50 mM Tris-HCl (pH 7.8)]. The reactions were started with ATP and stopped with $^1/_3$ volume of gel loading buffer after 2 min. We define the unit rate for autophosphorylation as 1 fmol of phospho-FixL (pmol of FixL)$^{-1}$ min^{-1}.

UV−Visible Absorption and Fluorescence Spectroscopies. UV−visible absorption spectra of FixL were measured with a Hitachi U-3000 spectrophotometer. The sample concentration was 5−10 μM. Fluorescence measurements of the met state of the I209W mutant excited by 296 nm radiation were taken with a Hitachi F-4010 fluorescence spectrometer with a sample concentration of 4 μM.

Resonance Raman Spectroscopy. Resonance Raman (RR) spectra were measured as previously described (*11*). Raman shifts were calibrated on the basis of the spectrum of indene with an absolute accuracy of $\pm$1 cm^{-1}. Excitation sources were a Kr^+ laser (Coherent) at 406.7 nm, a He−Cd laser (Kimmon) at 441.6 nm, and a Blue Solid-State Laser (Hitachi Metals, ICD-430) at 421 nm. The FixL concentration was 50 μM in 50 mM Tris-HCl (pH 8.0). Cyano-FixL, fluoro-FixL, and imidazole-bound FixL were prepared by equilibrating met-FixL with 1 mM KCN, 10 mM NaF, and 10 mM imidazole, respectively. Deoxy-FixL and carbon monoxy-FixL (CO-FixL) were prepared by filling the sample cell containing met-FixL with 100% N_2 gas and CO gas and then adding a few crystals of sodium dithionite, respectively. Oxy-FixL was prepared by adding a DTT solution (final concentration of 10 mM) to the sample cell containing met-FixL under the stream of 100% O_2 gas.

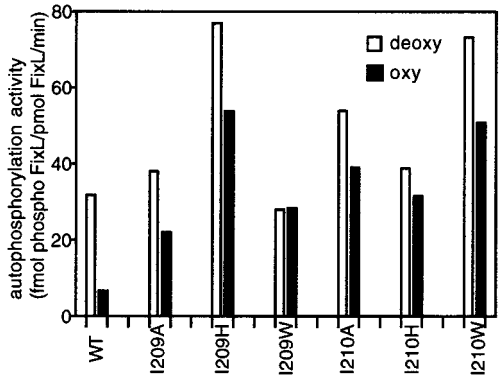

FIGURE 2: Autophosphorylation activity of WT FixL and its mutants in the deoxy and oxy states.

RESULTS

Autophosphorylation Activity of FixL and Its Mutants in Deoxy and Oxy States

Figure 2 shows the autophosphorylation activities of the wild type (WT) and mutants of FixL in the deoxy and oxy states at room temperature. The activities in the deoxy state of all proteins were more than 30 units, indicating that all mutants in the deoxy state were as active as WT FixL. However, the autophosphorylation activity of the mutants in the oxy state was significantly high, indicating that the autophosphorylation activities of the oxy forms of all the mutants are upregulated. In other words, the O_2 binding to the heme domain of the FixL mutants does not repress the autophosphorylation activity of their kinase domains. These results indicate that Ile209 and Ile210 play crucial roles in O_2 sensing by FixL. Since mutations of Ile209 and Ile210 have an effect on the O_2 sensing function of FixL possibly through structural changes in the heme pocket and/or in the heme iron coordination, we spectroscopically examined the structural changes with the mutations.

Absorption Spectroscopy

We previously reported UV−visible absorption spectra of the ferric, deoxy, and CO-bound forms of WT and I209A,

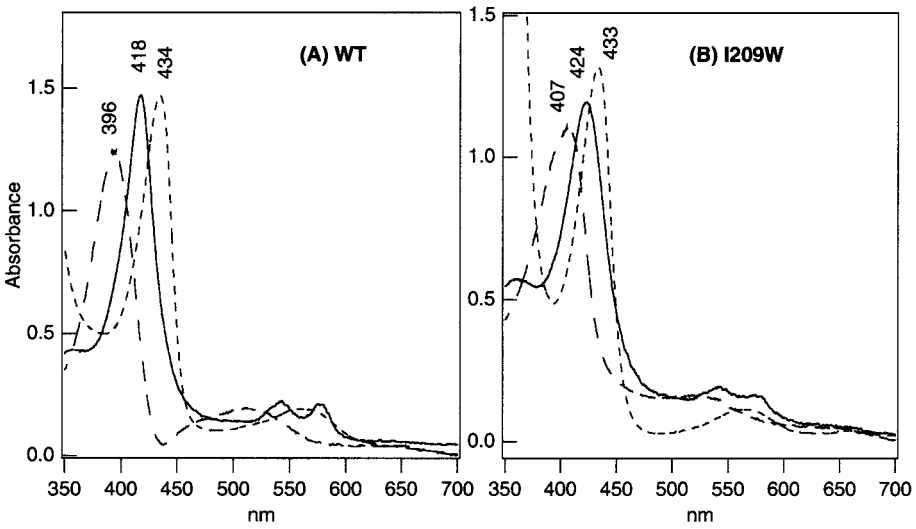

FIGURE 3: Absorption spectra of oxy (—), deoxy (- - -), and met (— —) states of WT FixL (A) and the I209W mutant (B). The buffer was 50 mM Tris-HCl (pH 8.0). The FixL concentrations were 10 μM (in the heme).

Table 1: Soret Band Peaks of UV−Visible Spectra in WT FixL and Its Mutants

	absorption peak (nm)			
	met	deoxy	oxy[a]	CO
WT	396	434	418	423
I209A	396	433	421	423
I209H	409	433	425	422
I209W[a]	407	433	424	423
I210A	398	433	427	423
I210H	414	433	421	423
I210W[a]	398	433	425	423

[a] This work. Other data are from ref *13*.

I209H, I210A, and I210H mutants of FixL (*13*). In the study presented here, the absorption spectra of the oxy complexes of all the proteins and those of I209W and I210W in the ferric, deoxy, and CO-bound states were also measured. As one of the examples, the absorption spectra of I209W are compared with the corresponding spectra of WT FixL in Figure 3. Absorption spectral data of all the mutants are summarized in Table 1. There was no difference in the positions of the Soret bands for the deoxy and CO-bound forms for all the mutants, as compared with those of the WT protein, whereas the absorption spectra in the ferric and oxy states were slightly different from those of the WT protein. Structural changes of FixL as a result of the Ile209 and Ile210 mutations were examined in more detail by the resonance Raman (RR) spectroscopic technique.

Resonance Raman Spectroscopy

Deoxy States. In the high-frequency region of the RR spectra, it is well-known that several bands serve as sensitive probes of the heme structures. The ν_3 (1460−1510 cm^{-1}) and ν_4 (1350−1380 cm^{-1}) bands are the spin state and the core size marker (ν_3) and the redox state maker of the heme (ν_4), respectively (*14*, *15*). The ν_3 and ν_4 bands of all FixLs in the deoxy state were observed at 1469−1471 and 1355−1356 cm^{-1}, respectively, indicating that the heme irons of all deoxy-FixLs are in a ferrous five-coordinated, high-spin state (5c-HS), as previously discussed for WT FixL (*16*). In the low-frequency region (Figure 4), the stretching (ν_{Fe-His})

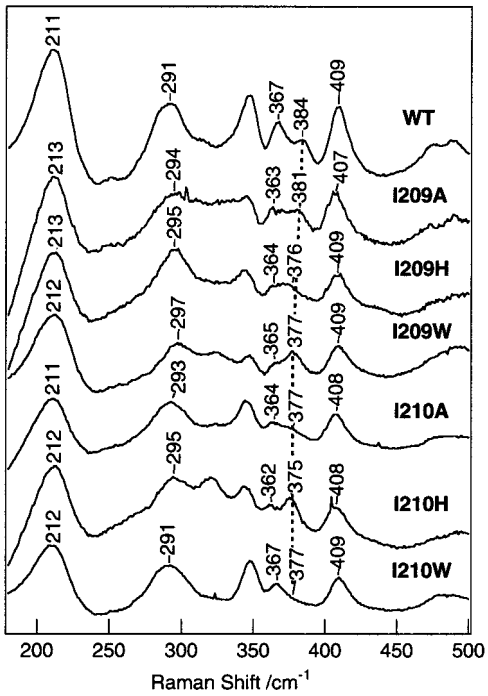

FIGURE 4: Resonance Raman spectra of FixL WT and its mutants in the deoxy state in the low-frequency region excited at 441.6 nm.

band derived from the Fe-proximal His194 bond (*17*) was observed at 211−213 cm^{-1} for every mutant in the RR spectra. Since the position of the ν_{Fe-His} band was not changed by the mutation, the Ile209 and Ile210 mutations hardly perturb the coordination structure of the heme-proximal His194 bond in the deoxy state.

The 384 cm^{-1} band of WT FixL could be assigned to the bending mode, $\delta(C_\beta C_c C_d)$, of the 6,7-propionates in the heme periphery (*18*−*20*). The band intensities of mutant FixLs were changed as compared with that of WT FixL. The intensity change suggests conformational changes of the heme propionate groups as a result of the mutation (*21*). On the other hand, Gottifried et al. reported that the 367 cm^{-1} band was sensitive to the strength of the hydrogen bond of the heme propionates (*22*); the band frequency is shifted

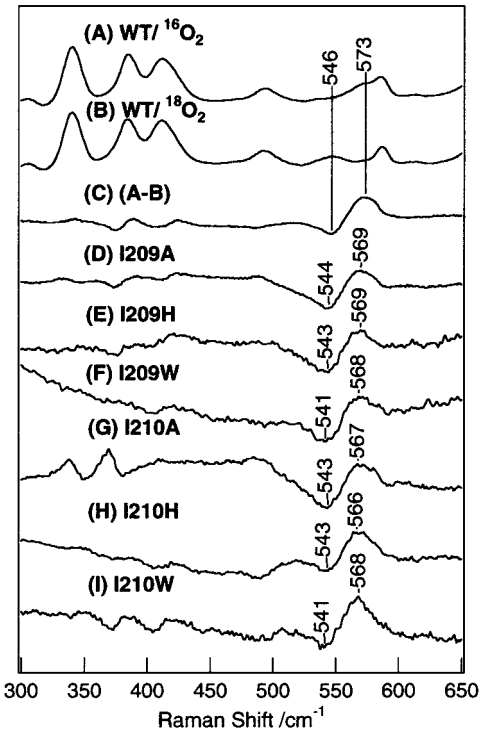

FIGURE 5: Resonance Raman spectra in the 300−650 cm^{-1} region for the $^{16}O_2$ (A) and $^{18}O_2$ (B) adducts of FixL WT and their difference spectrum (C) and difference spectra ($^{16}O_2$ minus $^{18}O_2$) of FixL mutants: I209A (D), I209H (E), I209W (F), I210A (G), I210H (H), and I210W (I) (421 nm excitation).

lower as the strength of the hydrogen bond decreases. The band frequencies of mutant FixLs were shifted lower than that of WT, except for I210W, indicating that the strength of the hydrogen bond of the heme propionates of those mutants was weakened by mutation. This result would be due to the conformational change of the heme propionates, consistent with the intensity change of the 384 cm^{-1} band of mutant FixLs.

O_2-Bound and CO-Bound Forms. The ν_3 and ν_4 bands of all FixLs in the oxy state were located at 1500−1502 and 1372−1375 cm^{-1}, respectively. The heme irons of all FixLs in the oxy state are in a six-coordinated, low-spin state (6c-LS). The Soret bands of the optical absorption spectra of all FixL mutants in the oxy state exhibited red shift, implying that these mutations yield structural changes in the heme moiety of the oxy complex of FixL. Figure 5 shows the RR spectra in the region of 300−650 cm^{-1} for the $^{16}O_2$ and $^{18}O_2$ adducts of WT FixL and its mutants. For assignment of the Fe−O_2 stretching (ν_{Fe-O_2}) band, the difference spectra between the $^{16}O_2$ and the $^{18}O_2$ adducts are also illustrated. The ν_{Fe-O_2} band of WT FixL for the $^{16}O_2$-bound adduct was observed at 573 cm^{-1}, in agreement with the frequencies previously observed (*11*). The ν_{Fe-O_2} frequencies are summarized in Table 2 together with frequencies of other iron-bound ligands (ν_{Fe-His}, ν_{Fe-CO}, and ν_{C-O}). It is noteworthy that the ν_{Fe-O_2} bands of all mutants are shifted to lower frequencies by 4−5 cm^{-1} compared to that of WT. It is reported that the ν_{Fe-O_2} band of heme proteins is sensitive to the steric effect in the heme pocket rather than the electrostatic field (*23*). Hence, the steric change to the iron-bound O_2 in the heme pocket of all mutants would be exerted by the mutation.

Table 2: Fe−Ligand Stretching Frequencies of FixL WT and Its Mutants

FixL	ν_{Fe-His} (cm^{-1})	ν_{Fe-O_2} (cm^{-1})	ν_{Fe-CO} (cm^{-1})	ν_{C-O} (cm^{-1})
WT	211	573	498	1962
I209A	213	569	495	1963
I209H	213	569	496	1962
I209W	212	568	494	1963
I210A	211	567	497	1961
I210H	212	566	496	1964
I210W	212	568	497	1965

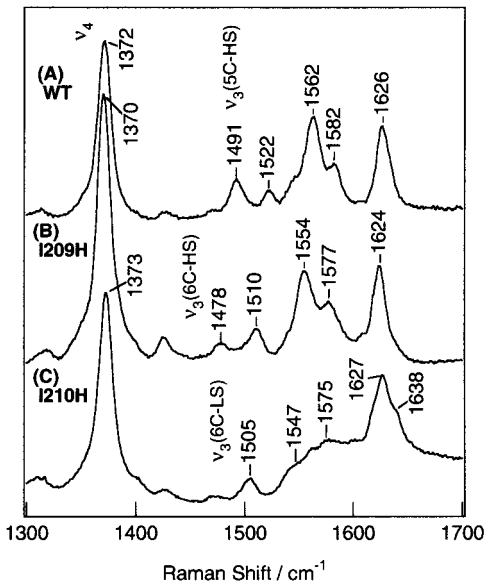

FIGURE 6: Resonance Raman spectra in the met state of FixL WT (A), I209H (B), and I210H (C) in the 1300−1700 cm^{-1} region at pH 8.0 (406.7 nm excitation).

On the other hand, the Fe−CO (ν_{Fe-CO}) and C−O (ν_{C-O}) stretching frequencies of FixL mutants were observed at almost the same value as those of the WT [ν_{Fe-CO} = 498 cm^{-1}; ν_{C-O} = 1962 cm^{-1} (*24*)] (see Table 2). It is well established that the ν_{Fe-CO} and ν_{C-O} frequencies of heme proteins are closely related and very sensitive to the electrostatic field of the heme pocket (*25*, *26*). Hence, these observations for the ν_{Fe-CO} and ν_{C-O} frequencies of FixL mutants imply that the electrostatic field in the heme pocket is not altered by the mutations of Ile209 and Ile210. Further, the steric effect on the iron-bound CO by the mutated residues is not clearly compared with that on the iron-bound O_2.

Ferric States. Figure 6 shows the RR spectra of FixLs of (A) WT, (B) I209H, and (C) I210H in the ferric state in the region of 1300−1700 cm^{-1}. The RR spectra of these mutants are different from that of the WT protein. The marker bands (ν_3 and ν_4) of I209A, I210A, and I210W were similar in position to those of WT, while those of I209W were the same as those of I209H.

On the basis of the features of the RR and optical absorption spectra (see Table 1), the FixL mutants in the ferric state can be classified into three groups: the WT, I209H, and I210H groups. The ν_3 band of the WT group (WT, I209A, I210A, and I210W) was observed at 1491 cm^{-1} (*21*), indicating that the heme iron is in a ferric 5c-HS.

The ν_3 band of the I209H group (I209H and I209W) is located at 1478 cm^{-1}, indicating that the ferric heme iron is

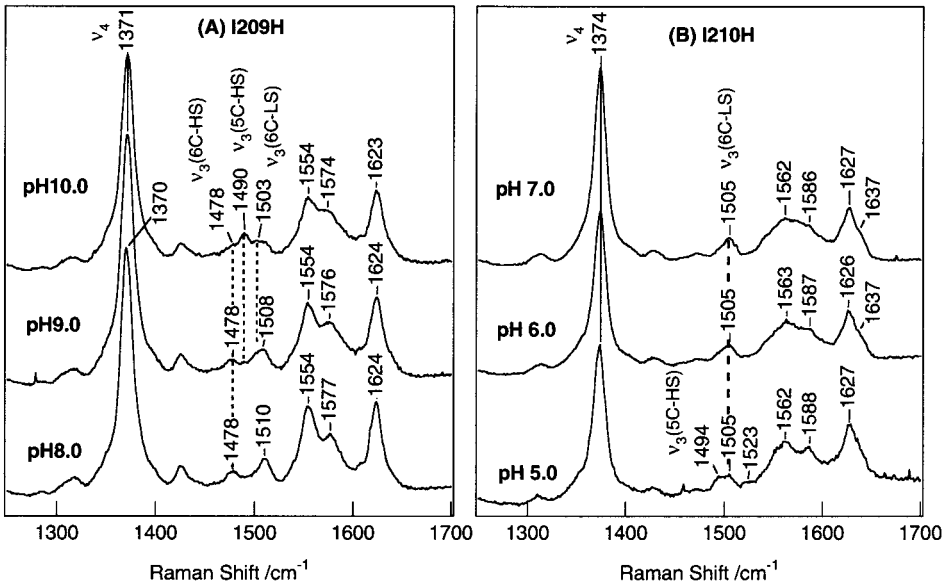

FIGURE 7: Resonance Raman spectra in the met state of I209H (A) and I210H (B) at the indicated pH.

in a 6c-HS. This assignment was supported by the observation of the fluorine complex (ν_3 band at 1475 cm^{-1}) of WT FixL with a 6c-HS heme. As the pH is increased, the intensity of the 1478 cm^{-1} band decreased with the concomitant appearance of the new ν_3 bands at 1490 cm^{-1} (5c-HS) and 1503 cm^{-1} (6c-LS) (see Figure 7A). The 1503 cm^{-1} band can be assigned to the 6c-LS FixL$-OH^-$ complex (*21*). This pH dependence of the spectra is explained as follows. The iron-bound H_2O at neutral pH is ionized to OH^- as the pH is raised. Hence, we concluded that H_2O is the candidate with the most potential as a sixth ligand of the I209H group at neutral pH. This result indicates that the hydrophobicity of the heme pocket is decreased by the mutation at position 209.

In the case of the I210H group, the ν_3 band was observed at 1505 cm^{-1}. The spectral similarity to the CN-bound (ν_3 = 1503 cm^{-1}) and the imidazole-bound (ν_3 = 1505 cm^{-1}) forms of WT FixL indicates that the heme iron of I210H is in the 6c-LS. In addition, the pH dependence of the spectrum is also identical for I210H (see Figure 7B) and the imidazole complex of WT FixL. We could suggest that the imidazole of the introduced His210 internally coordinates to the iron as a sixth ligand to form the 6c-LS heme. One of the possible reasons that I210H has the bis-His coordinated heme, but I209H does not, could be the difference in the hydrophobicity of the heme pocket between I209H and I210H. The heme pocket of I210H is hydrophobic, similar to that of WT, because Ile209 is still located near the heme iron, and H_2O could not come in the heme pocket. Hence, the imidazole of His210 could be coordinated to the heme iron.

DISCUSSION

Structural Changes in the Heme Pocket of FixL as a Result of Mutation. The distal heme pocket of the WT FixL is hydrophobic, and no water molecule was present there in the ferric state (*11*). Therefore, the presence of H_2O at the sixth coordination site of the heme iron in I209H and I209W mutants indicates that the hydrophobicity in the heme pocket is decreased by the Ile209 mutations. However, despite such a change in the hydrophobicity, the ν_{Fe-CO} and ν_{C-O} frequencies, which are very sensitive to the electrostatic field in the heme pocket, of the CO-bound form of FixL were not affected by the replacement of Ile with His (I209H). If the His209 side chain of the I209H mutant is located near the heme iron as for Ile209 of WT, the ν_{Fe-CO} and ν_{C-O} frequencies of I209H should be shifted about 19−20 cm^{-1} due to the change in the electrostatic field caused by the introduced His209 according to the result of the Mb-CO mutants (*27*, *28*). However, this is not true for the position 209 mutation of FixL, and the electrostatic field at the iron-bound CO induced by the distal residue is not changed by the Ile209 mutation. This result could be explained by the elongation of the distance between the position 209 side chain and the heme iron by the replacement of Ile209. Due to its elongation, the extent of the electrostatic effect of the His209 side chain on the heme iron would decrease and the electrostatic field at the iron-bound CO would be almost similar to that in the WT. The elongation would be accomplished by the movement of the imidazole group of His209 away from the heme pocket.

Trp209 in the I209W mutant may also move away from the heme pocket. The conformational change induced by the mutation would be supported by the fluorescence measurements via UV excitation, in which the position of the fluorescence peak (λ_{max}) depends on the local environment of the Trp residue (*29*). Since WT FixL does not contain any Trp residue, the fluorescence of I209W originates from the introduced Trp209 residue. The λ_{max} values of I209W were observed at 340 nm (data not shown), showing that the Trp209 side chain is located in a relatively solvent-accessible environment (*29*).

Because the heme pocket is opened by these conformational change, the O_2 ligand also coordinates to the heme iron in I209H, I209W, and I209A with less steric hindrance, compared with the coordination in WT FixL, judged from the observation that the ν_{Fe-O_2} band was shifted in the lower-field direction by the Ile209 mutations. The observation is comparable to those in comprehensive studies on Mb mutants (*23*), where relationships between the ν_{Fe-O_2} frequency and the Fe−O−O angle are observed in the oxy complexes of

L29F Mb (568 cm^{-1} and 120°, respectively), of WT Mb (571 cm^{-1} and 118°, respectively), and of L29W Mb (574 cm^{-1} and 111°, respectively). The lower shift of the ν_{Fe-O_2} frequency indicates that the O_2 coordinates to the heme iron in a more linear fashion by diminishing the steric hindrance. On the other hand, the steric effect on the iron-bound CO of FixL did not appear clearly. This difference between O_2 and CO ligands in the steric effect might be due to the difference between the Fe−O−O and Fe−C−O angles.

On the other hand, although the side chain of Ile210 faces outside of the protein molecule (see Figure 1), the mutational effect of Ile210 on the ligand coordination was apparently identical to that of Ile209 (see Figure 5 and Table 2). This observation suggests that the protein conformation around Ile210 is highly flexible, and consequently, the imidazole group of the introduced His210 in I210H coordinates to the heme iron as an internal sixth ligand in the ferric state.

In the study presented here, we can reveal the mutational effects of Ile209 and Ile210, located on the F/G loop of FixL, on the structures of the iron−ligand coordination. On the basis of these results, we likely conclude that Ile209 and Ile210 are highly flexible and sterically interact with the O_2 ligand. This conclusion is very consistent with the suggestions derived from the temperature factors of the main chain of these residues which were crystallographically examined (*11*).

Roles of Ile209 and Ile210 in the O_2 Sensing Mechanism. All the mutants of FixL we examined in this study exhibited the upregulated autophosphorylation activity in the oxy state, and therefore, the O_2 sensing mechanism is disrupted by the mutations at positions 209 and 210. It is likely to suggest that Ile209 and Ile210 are involved in the O_2 sensing of FixL. On the other hand, the side chains of Ile209 and Ile210 are highly flexible and appear to be easily changed from their original position upon O_2 binding. Combination of these implications allows us to propose that the O_2 sensing of RmFixL would be initiated by the steric interaction of Ile209 and/or Ile210 when O_2 binds to the heme iron. The O_2 association with the heme iron would change the conformations of Ile209 and Ile210, and the conformational change of these residues would induce structural changes in the F/G loop, which might be transmitted to the kinase domain for inactivation of the catalytic site by intramolecular signal transduction.

On the basis of the crystal structures of ferric and ferric−CN^- complexes of BjFixLH, Gong et al. proposed the O_2 sensing mechanism, in which O_2 binding to the heme iron makes the heme plane flatten, and eventually causes the rearrangement of the hydrogen bond network between the heme propionates and the residues (Arg206 and His214) on the F/G loop to inactivate the kinase activity (*9*). However, even in the mutants at positions 209 and 210, which are upregulated, the heme plane should be flattened upon O_2 binding to the heme iron, and the hydrogen bond network should be rearranged because the interaction of residue 209 (or 210) with the O_2-bound heme is diminished by the mutation. In addition, we noted that the intensity of the $\delta(C_\beta C_c C_d)$ band of the heme propionate was different among the mutants of FixL and the 367 cm^{-1} band, which is sensitive to the strength of the hydrogen bond of the propionates, of the WT was shifted lower in the mutants, suggesting structural changes at this site as a result of the Ile209 and Ile210 mutations. Despite such structural changes at the heme propionate, the autophosphorylation activity in the deoxy state was not altered. Therefore, the rearrangement of the hydrogen bond network between the heme propionate and residues in the F/G loop might be a result of movement of the F/G loop caused by the structural changes at the Ile209 and/or Ile210 site.

Most recently, Gong et al. reported the crystal structures of the oxy, NO, and imidazole complexes of BjFixLH (*10*). In this report, they discussed the O_2 sensing mechanism previously proposed, in which the hydrogen-bonding rearrangement of the heme propionate is an initial step. However, we have noticed in their report that the side chain of Ile209 (Ile215 in BjFixLH) is largely changed in its position with respect to the accommodation of O_2 to allow the hydrogen-bonding interaction between the iron-bound O_2 and guanidyl group of Arg214 (Arg220 in BjFixLH). The crystallographic data appear to significantly support our results of the Ile209 and Ile210 mutagenesis of FixL. In addition, Perutz et al. discussed in their review the possibility that the steric effect between the iron-bound ligand and three distal residues (corresponding to Ile209, Leu230, and Val232 in RmFixL) may be important to the signal transduction of FixL (*12*). We proved that the interaction between Ile209 (and/or Ile210) and the iron-bound O_2 ligand is essential to the O_2 sensing mechanism of FixL.

ACKNOWLEDGMENT

We are grateful to Prof. Teizo Kitagawa (Institute for Molecular Science) for help in using the 421 nm laser on the resonance Raman measurement of oxy-FixL.

REFERENCES

1. Stock, J. B., Ninfa, A. J., and Stock, A. M. (1989) *Microbiol. Rev. 53*, 450−490.
2. Gilles-Gonzalez, M. A., Ditta, G. S., and Helinski, D. R. (1991) *Nature 350*, 170−172.
3. Fisher, R. F., and Long, S. R. (1992) *Nature 357*, 655−660.
4. Monson, E. K., Weinstain, M., Ditta, G. S., and Helinski, D. R. (1992) *Proc. Natl. Acad. Sci. U.S.A. 89*, 4280−4284.
5. Lois, A. F., Weinstein, M., Ditta, G. S., and Helinski, D. R. (1993) *J. Bacteriol. 175*, 1103−1109.
6. Gilles-Gonzalez, M. A., and Gonzalez, G. (1993) *J. Biol. Chem. 268*, 16293−16297.
7. Gilles-Gonzalez, M. A., Gonzalez, G., and Perutz, M. F. (1994) *Biochemistry 33*, 8067−8073.
8. Gilles-Gonzalez, M. A., Gonzalez, G., and Perutz, M. F. (1995) *Biochemistry 34*, 232−236.
9. Gong, W., Hao, B., Mansy, S. S., Gonzalez, G., Gilles-Gonzalez, M. A., and Chan, M. K. (1998) *Proc. Natl. Acad. Sci. U.S.A. 95*, 15177−15182.
10. Gong, W., Hao, B., and Chan, M. K. (2000) *Biochemistry 39*, 3955−3962.
11. Miyatake, H., Mukai, M., Park, S.-Y., Adachi, S., Tamura, K., Nakamura, H., Tsuchiya, T., Iizuka, T., and Shiro, Y. (2000) *J. Mol. Biol. 301*, 415−431.
12. Perutz, M. F., Paoli, M., and Lesk, A. M. (1999) *Chem. Biol. 6*, R291−R297.
13. Nakamura, H., Saito, K., Ito, E., Tamura, K., Tsuchiya, T., Nishigaki, K., Shiro, Y., and Iizuka, T. (1998) *Biochem. Biophys. Res. Commun. 247*, 427−431.
14. Spiro, T. G., and Li, X.-Y. (1988) in *Biological Applications of Raman Spectroscopy* (Spiro, T. G., Ed.) Vol. III, pp 1−37, Wiley, New York.
15. Kitagawa, T. (1988) in *Biological Applications of Raman Spectroscopy* (Spiro, T. G., Ed.) Vol. III, pp 97−131, Wiley, New York.

16. Tamura, K., Nakamura, H., Tanaka, Y., Oue, S., Tsukamoto, K., Nomura, M., Tsuchiya, T., Adachi, S., Takahashi, S., Iizuka, T., and Shiro, Y. (1996) *J. Am. Chem. Soc. 118*, 9434−9435.
17. Teraoka, J., and Kitagawa, T. (1981) *J. Biol. Chem. 256*, 3969−3977.
18. Feis, A., Marzocchi, M. P., Paoli, M., and Smulevich, G. (1994) *Biochemistry 33*, 4577−4583.
19. Hu, S., Morris, I. K., Singh, J. P., Smith, K. M., and Spiro, T. G. (1993) *J. Am. Chem. Soc. 115*, 12446−12458.
20. Smulevich, G., Hu, S., Rodgers, K. R., Goodin, D. B., Smith, K. M., and Spiro, T. G. (1996) *Biospectroscopy 2*, 365−376.
21. Lukat-Rodgers, G. S., Rexine, J. L., and Rodgers, K. R. (1998) *Biochemistry 37*, 13543−13552.
22. Gottfried, D. S., Peterson, E. S., Sheikh, A. G., Wang, J., Yang, M., and Friedman, J. M. (1996) *J. Phys. Chem. 100*, 12034−12042.
23. Hirota, S., Li, T., Philips, G. N., Jr., Olson, J. S., Mukai, M., and Kitagawa, T. (1996) *J. Am. Chem. Soc. 118*, 7845−7846.
24. Miyatake, H., Mukai, M., Adachi, S., Nakamura, H., Tamura, K., Iizuka, T., and Shiro, Y. (1999) *J. Biol. Chem. 274*, 23176−23184.
25. Tsubaki, M., Srivastava, R. B., and Yu, N.-T. (1982) *Biochemistry 21*, 1131−1140.
26. Yu, N.-T., Kerr, E. A., Ward, B., and Chang, C. K. (1983) *Biochemistry 22*, 4534−4540.
27. Nakashima, S., Kitagawa, T., and Olson, J. S. (1998) *Chem. Phys. 228*, 323−336.
28. Li, T., Quillin, M. L., Phillips, G. N. J., and Olson, J. S. (1994) *Biochemistry 33*, 1433−1446.
29. Li, J., Szittner, R., and Meighen, E. A. (1998) *Biochemistry 37*, 16130−16138.

BI001184X